XV Latin American Symposium on High Energy Physics
Mexico City, nov 5, 2024

AGENCIA ESPACIAL DEL PERU CONIDA

UNIVERSIDAD NACIONAL DE INGENIERIA SCIENTIA ET LABOR LIMA 1876 PERU

ProCIENCIA

CONCYTEC CONSEJO NACIONAL DE CIENCIA, TECNOLOGÍA E INNOVACIÓN

Development of muon tomography for non-invasive studies of geophysical objects

J. BAUTISTA LEON [1]

C. CASTROMONTE [1], L. OTINIANO [2]

(1) Universidad Nacional de Ingeniería
(2) Comisión Nacional de Investigación y Desarrollo Aeroespacial (CONIDA)

MOTIVATION

- Peru is a country with many archaeological sites and mysteries about many cultures. In addition, there are many geophysical objects in different regions. Muography is a technique used to study these important sites, however, this is the first time that Peru has developed a muography project.

Secret door at Machu Picchu (Cusco, Peru)

Misti volcano (Arequipa, Peru)

HISTORY

- Muography began in 1965 when L. Álvarez and his colleagues used this technique to analyze the Kefren pyramid, they concluded that there are no hidden chambers. In 2017, a chamber was detected in the Great Pyramid of Giza.

Luis Walter Álvarez (1965)

Equipment detected a chamber at the base of the Great Pyramid of Giza (2017)

COSMIC RAYS

- Cosmic rays reaching the atmosphere are mainly protons and alpha particles (98%). The remainder is made up of electrons and ionized heavy particles. These are called primary particles.
- EAS or secondary particles have three components: electromagnetic (photons, electrons and positrons); hadronic (kaons, pions, neutrons and protons) and muonic (muons and muon neutrinos).

$$
\begin{aligned}
K^+ &\rightarrow \mu^+ + \nu_\mu && 63.56\% \\
K^+ &\rightarrow \pi^+ + \pi^0 && 20.67\% \\
K^+ &\rightarrow \pi^+ + \pi^+ + \pi^- && 5.58\% \\
\pi^+ &\rightarrow \mu^+ + \nu_\mu && 99.9\%
\end{aligned}
\qquad (1)
$$

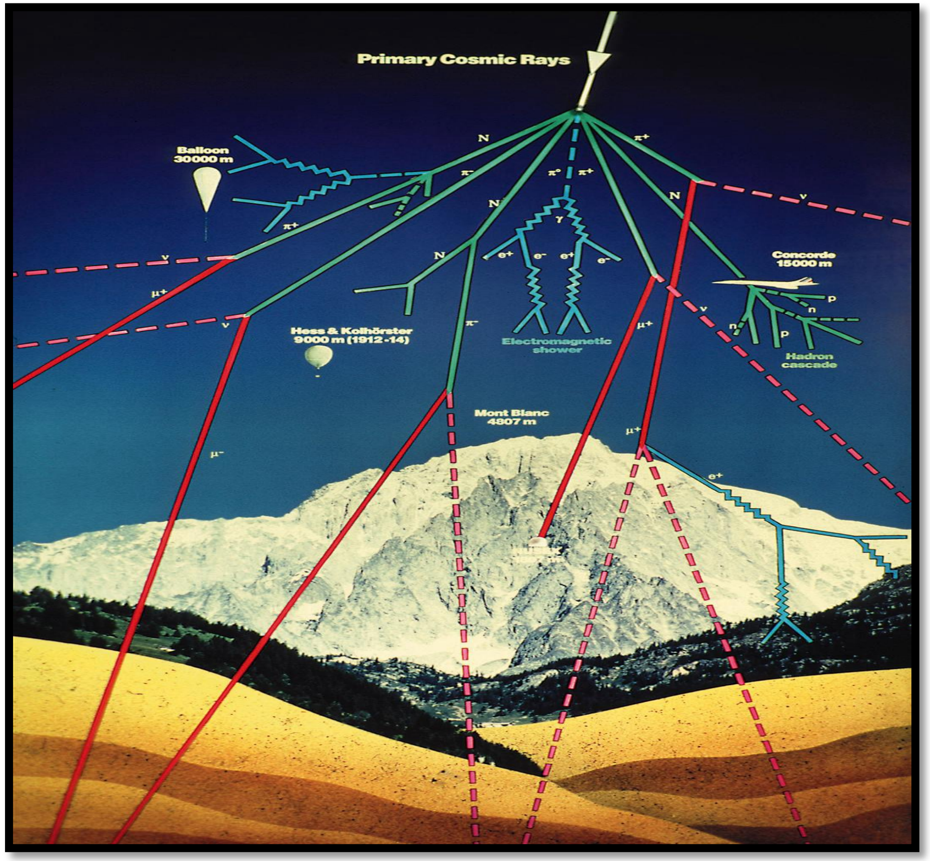

WHY MUONS?

- Muons are:
  - Charged Particles
  - ~200 times the mass of the electron (105.7 MeV/c^2)
- They fall on the earth with a constant open sky flux on the azimuthal angle from which it is measured.
- There is a strong dependence on the zenith angle at which the muons arrive, as well as the height (relative to sea level) from which they are detected.

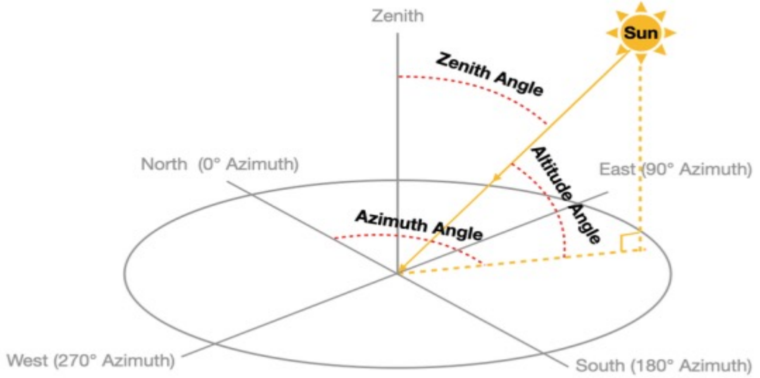

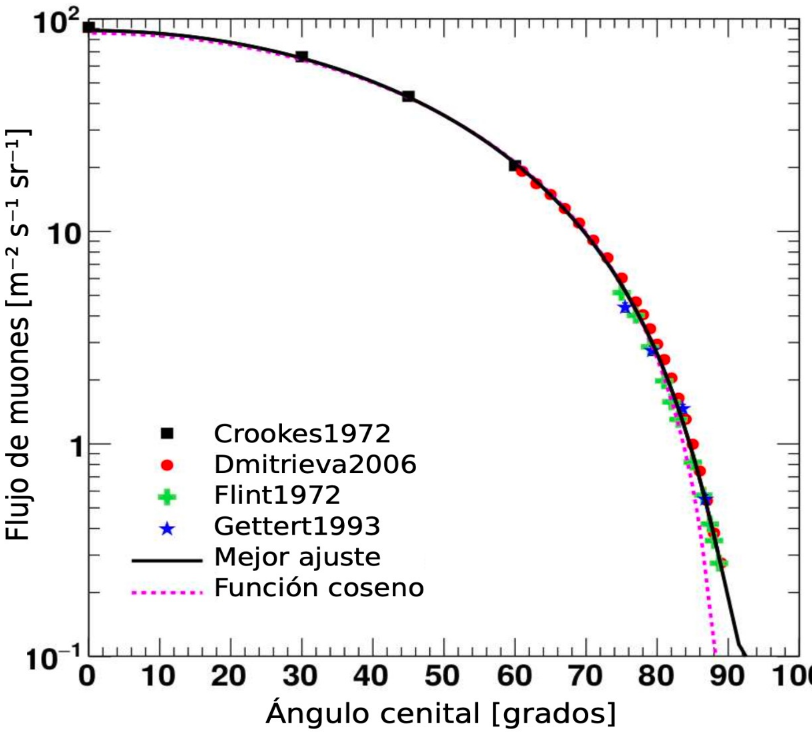

Dependence of the integral muon flux at sea level on the zenith angle

Pena-Rodriguez, J. (2021). *Diseño y calibración de un telescopio de muones híbrido para estudios vulcanológicos* (Doctoral dissertation, Universidad Industrial de Santander).

MUOGRAPHY

- Muography is based on the measurement of the atmospheric muon flux passing through an object in different directions. The fraction of muons that manage to pass through the material is determined by the *opacity*:

$$\rho(L) = \int_L \rho(x)dx \qquad (2)$$

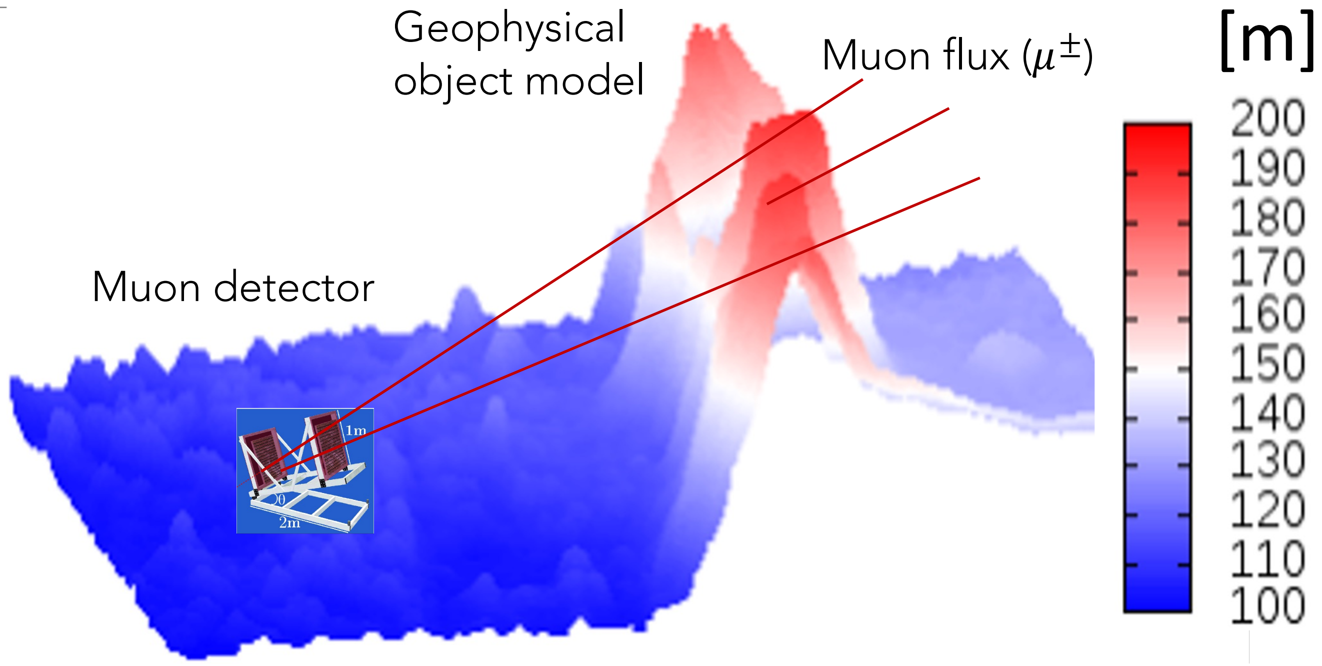

- The opacity ρ is deduced by the attenuation of the muon flux, Φ, measured after passing through the object under study, compared with the incident flux Φ_0 , measured under open sky conditions.

TOMOGRAPH

- A hodoscope is an instrument that determines the trajectory of charged particles passing through it, and is made up of two or more detection planes.
- Each of these is made up of two rows of scintillator bars ("channels"). It determines a position, on the front panel as well as the rear panel.

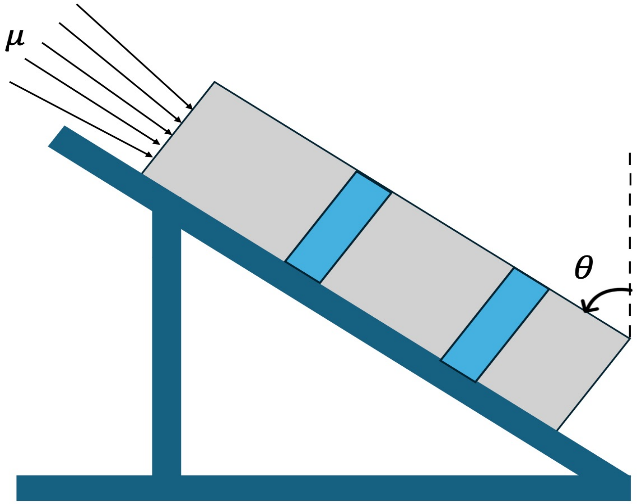

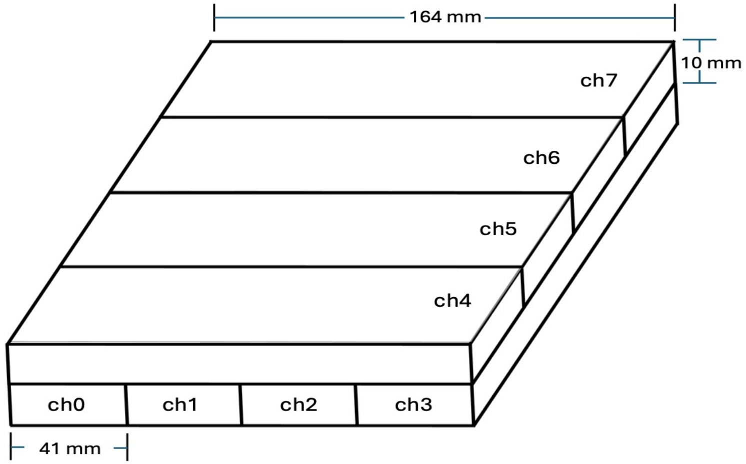

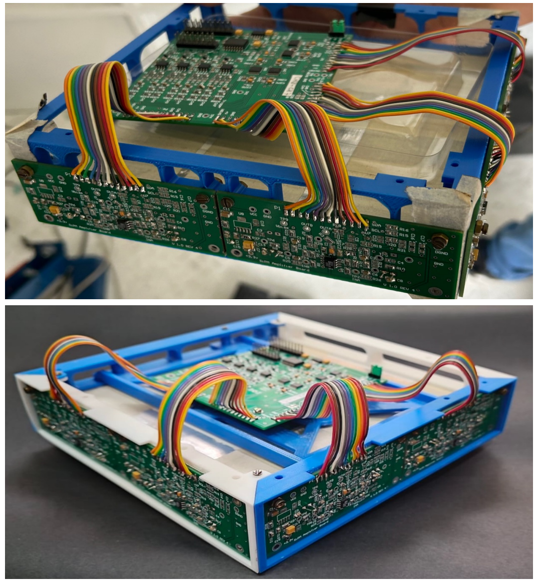

Diagram of the bars and panels positions in the detector (left) and the detection planes photographs (right). (UNI-CONIDA muon tomograph, project 139-2017 FONDECYT).

TEST SITE

Map of the test site, Universidad Nacional de Ingeniería (left). Detector pointing to open sky (right).

DETECTION PROCESS

- When a charged particle interacts with the scintillator bar, it emits a photon which is guided by the optical fiber towards the SiPM, generating a pulse that is subsequently digitized.

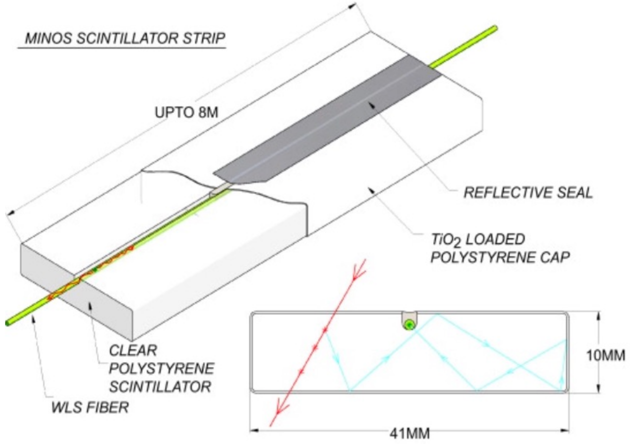

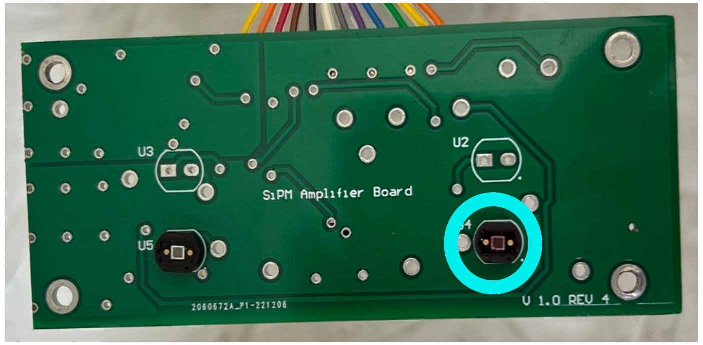

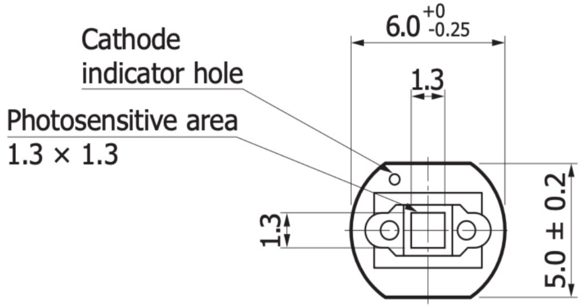

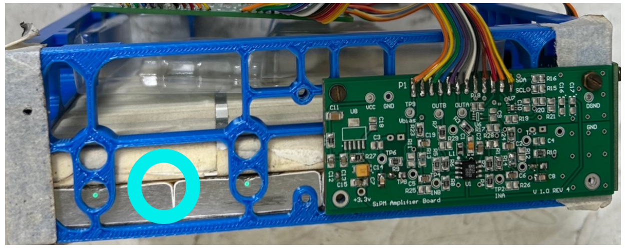

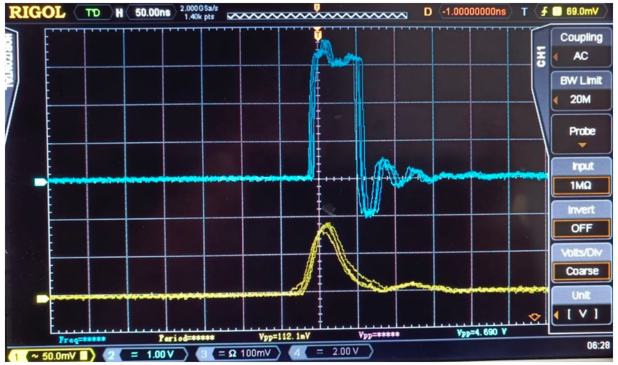

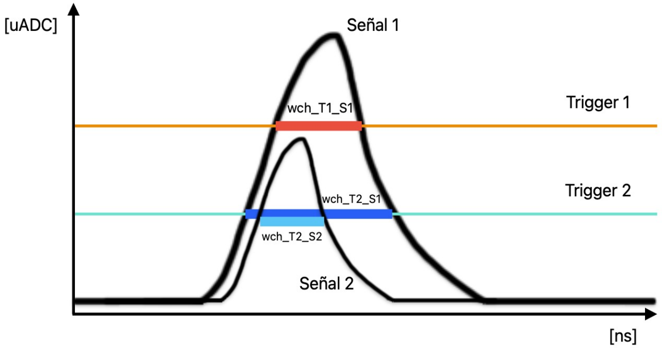

OPTICAL ADAPTATION

- Polishing of scintillation bars with micrometric grains and coupling with optical glue.

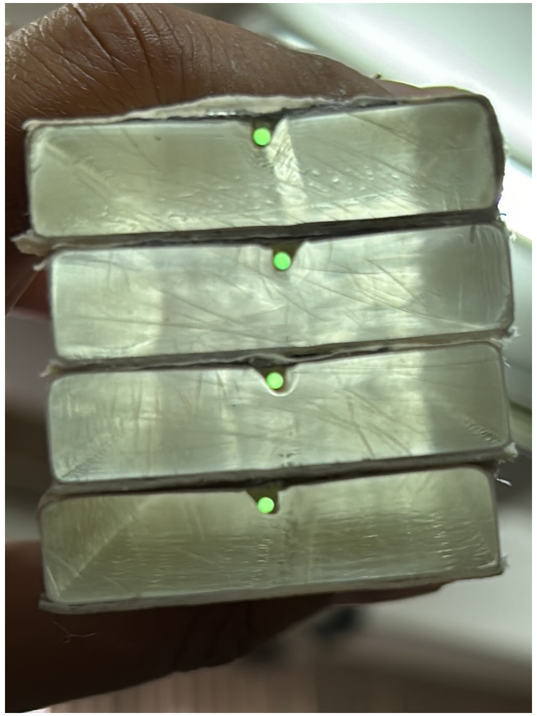

CHANNELS GEOMETRIC ARRANGEMENT

- Detector acceptance $T(r_{m,n})$ has a strong dependance on its geometry; each pair of bars in front panel determine a pixel m , in an analogous way, each pair of bars in rear panel determine a pixel n. Also, each pair of pixels m and n determine a distance $r_{m,n}$ and trajectory.

$$T(r_{m,n}) = S(r_{m,n}) \times \delta\Omega(r_{m,n}); \qquad \delta\Omega = \frac{4A}{r_{m,n}^2} \quad (3)$$

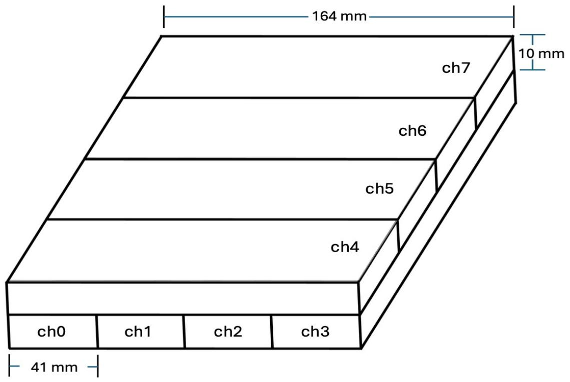

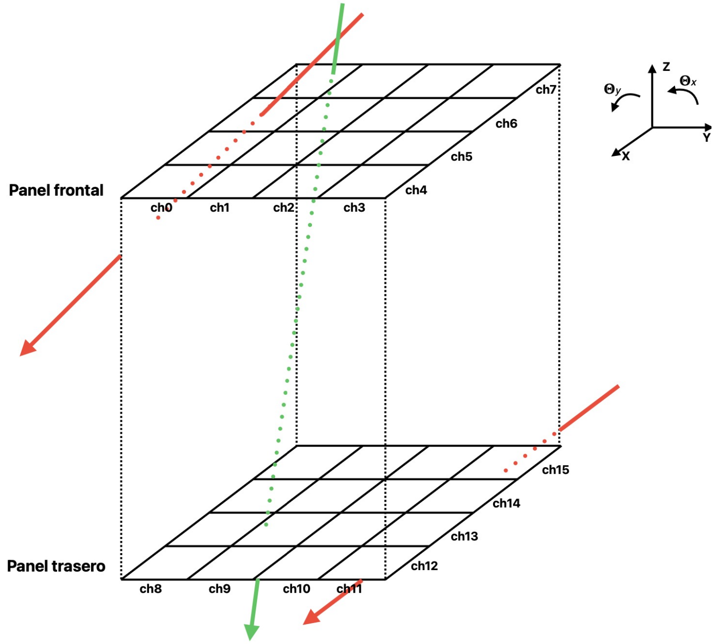

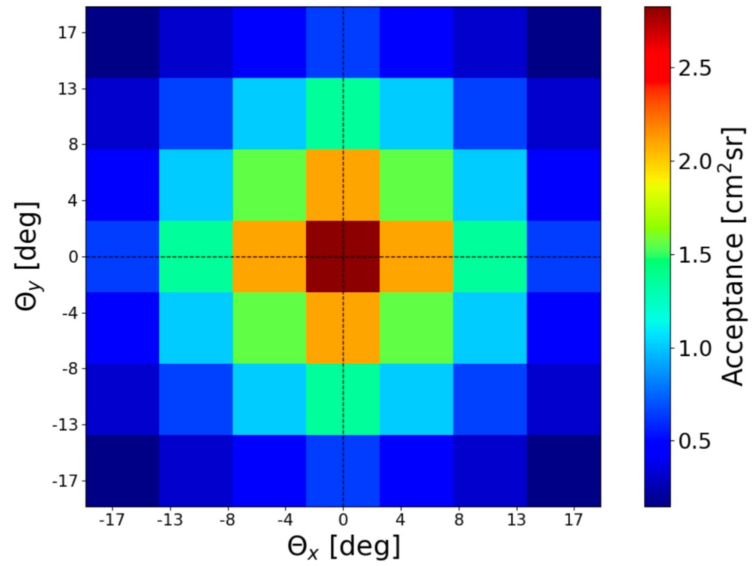

Arrangement of the detector channels (left) and their geometric acceptance (right).

DATA COLLECTION

- Electronic data processing is carried out through two electronic modules: a board where the detector drivers are located, and another (Pitaya network) where the Debian operating system is installed.

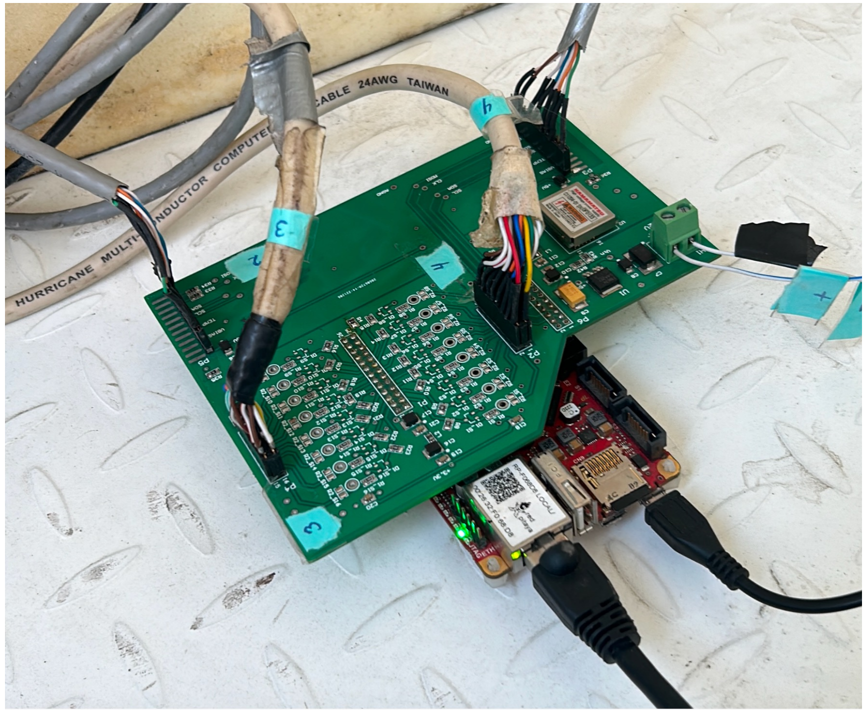

Pitaya Network (red board) conecting with drivers board (green board).

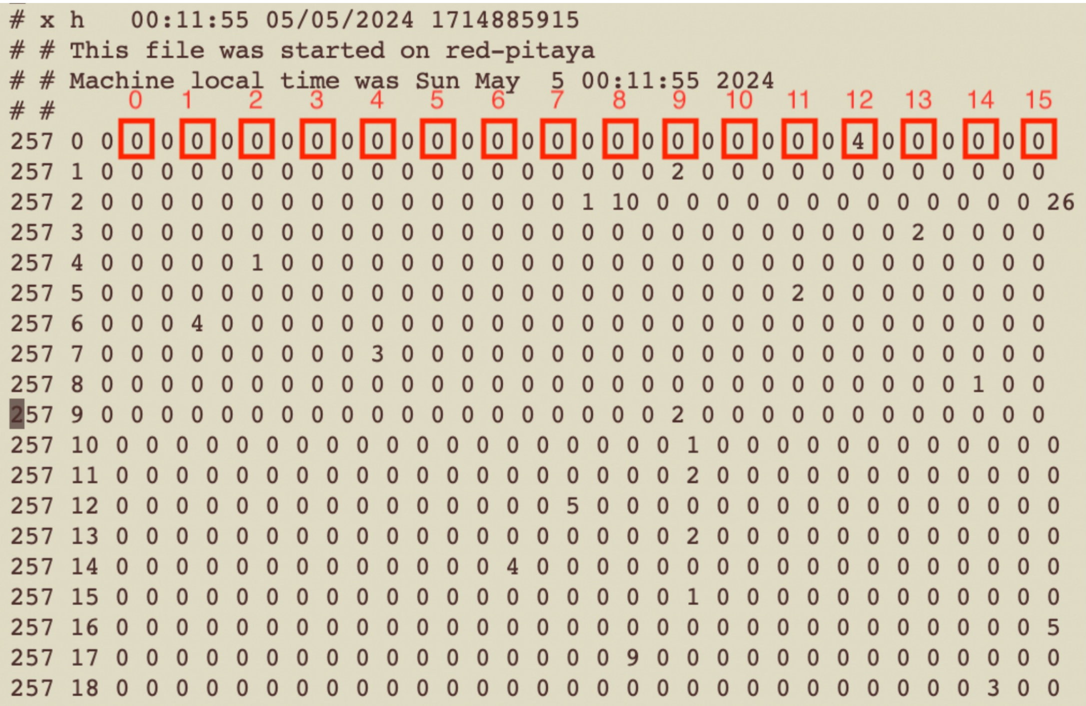

```
# x h   00:11:55 05/05/2024 1714885915
# # This file was started on red-pitaya
# # Machine local time was Sun May  5 00:11:55 2024
# #     0 1 2 3 4 5 6 7 8 9 10 11 12 13 14 15
257 0 0 0 0 0 0 0 0 0 0 0 0 0 0 0 0 0 0 0 0 0 0 0 0 0 0 4 0 0 0 0 0 0
257 1 0 0 0 0 0 0 0 0 0 0 0 0 0 0 0 0 0 0 0 2 0 0 0 0 0 0 0 0 0 0 0 0
257 2 0 0 0 0 0 0 0 0 0 0 0 0 0 0 0 0 1 10 0 0 0 0 0 0 0 0 0 0 0 0 0 26
257 3 0 0 0 0 0 0 0 0 0 0 0 0 0 0 0 0 0 0 0 0 0 0 0 0 0 0 0 2 0 0 0 0
257 4 0 0 0 0 0 1 0 0 0 0 0 0 0 0 0 0 0 0 0 0 0 0 0 0 0 0 0 0 0 0 0 0
257 5 0 0 0 0 0 0 0 0 0 0 0 0 0 0 0 0 0 0 0 0 0 0 0 2 0 0 0 0 0 0 0 0
257 6 0 0 0 4 0 0 0 0 0 0 0 0 0 0 0 0 0 0 0 0 0 0 0 0 0 0 0 0 0 0 0 0
257 7 0 0 0 0 0 0 0 0 0 3 0 0 0 0 0 0 0 0 0 0 0 0 0 0 0 0 0 0 0 0 0 0
257 8 0 0 0 0 0 0 0 0 0 0 0 0 0 0 0 0 0 0 0 0 0 0 0 0 0 0 0 0 0 1 0 0
257 9 0 0 0 0 0 0 0 0 0 0 0 0 0 0 0 0 0 0 0 2 0 0 0 0 0 0 0 0 0 0 0 0
257 10 0 0 0 0 0 0 0 0 0 0 0 0 0 0 0 0 0 0 0 1 0 0 0 0 0 0 0 0 0 0 0 0
257 11 0 0 0 0 0 0 0 0 0 0 0 0 0 0 0 0 0 0 0 2 0 0 0 0 0 0 0 0 0 0 0 0
257 12 0 0 0 0 0 0 0 0 0 0 0 0 0 0 0 5 0 0 0 0 0 0 0 0 0 0 0 0 0 0 0 0
257 13 0 0 0 0 0 0 0 0 0 0 0 0 0 0 0 0 0 0 0 2 0 0 0 0 0 0 0 0 0 0 0 0
257 14 0 0 0 0 0 0 0 0 0 0 0 0 0 4 0 0 0 0 0 0 0 0 0 0 0 0 0 0 0 0 0 0
257 15 0 0 0 0 0 0 0 0 0 0 0 0 0 0 0 0 0 0 0 1 0 0 0 0 0 0 0 0 0 0 0 0
257 16 0 0 0 0 0 0 0 0 0 0 0 0 0 0 0 0 0 0 0 0 0 0 0 0 0 0 0 0 0 0 0 5
257 17 0 0 0 0 0 0 0 0 0 0 0 0 0 0 0 0 0 9 0 0 0 0 0 0 0 0 0 0 0 0 0 0
257 18 0 0 0 0 0 0 0 0 0 0 0 0 0 0 0 0 0 0 0 0 0 0 0 0 0 0 0 0 0 3 0 0
```

Dataset format.

DETECTED EVENTS

- The first part of data analysis consists of verifying the status of the channels.

ROOT
Data Analysis Framework

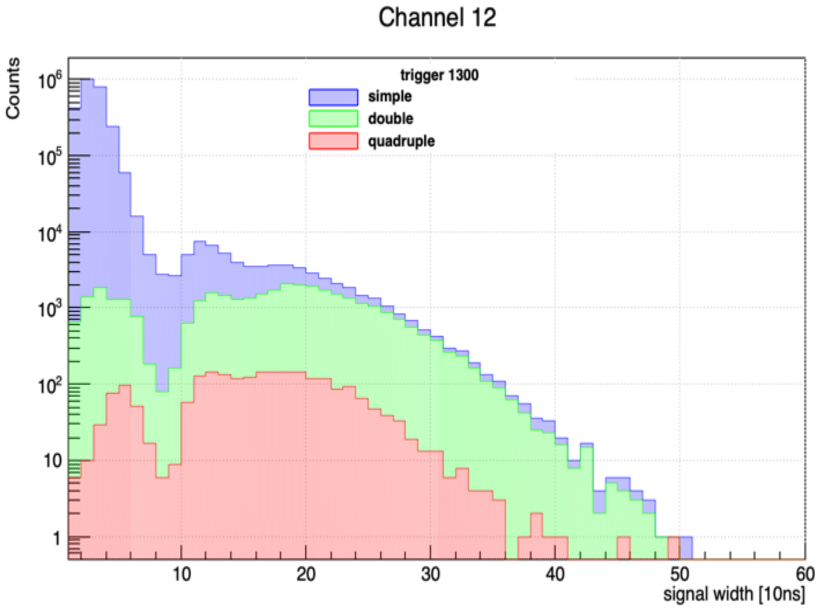

Data comparison in coincidence.

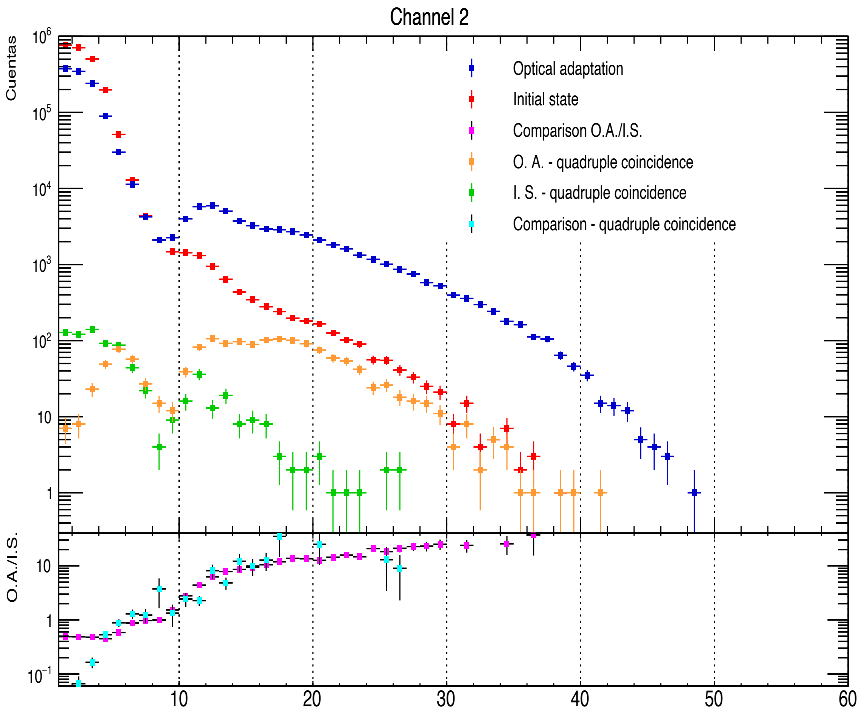

Data comparison after optical adaptation.

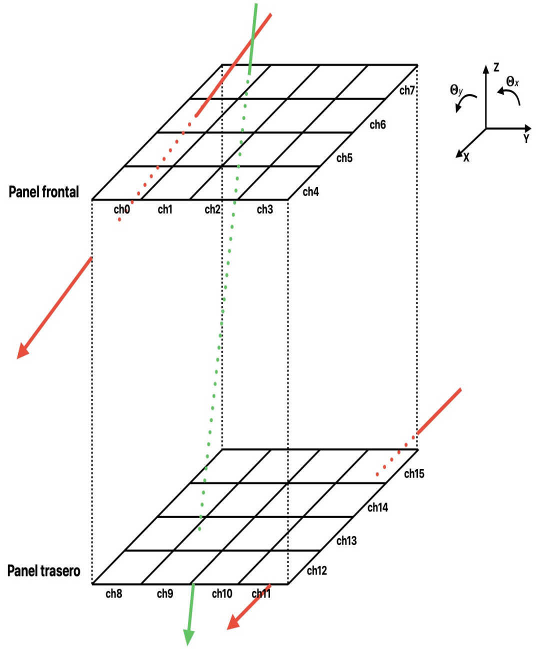

ATMOSPHERIC MUON FLUX

- The atmospheric muon flux detected is defined as:

$$I = \frac{N}{\Delta t \times T} \quad (3)$$

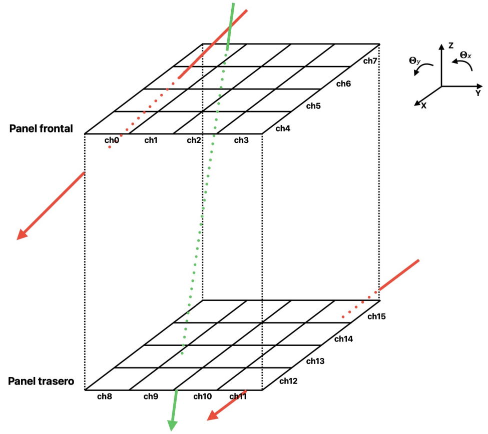

- Each detector angle is defined according to its inclination, with respect to central angle, given the equation:

$$\theta = \cos^{-1}\left(\frac{\frac{(n_2-n_1)d}{D}\operatorname{sen}\Theta + \cos\Theta}{\sqrt{\left(\frac{(m_2-m_1)d}{D}\right)^2 + \left[\frac{(n_2-n_1)d}{D}\cos\Theta - \operatorname{sen}\Theta\right]^2 + \left[\frac{(n_2-n_1)d}{D}\operatorname{sen}\Theta - \cos\Theta\right]^2}}\right) \quad (4)$$

ATMOSPHERIC MUON FLUX

- The value of the exponent in the cosine approaches 2 :

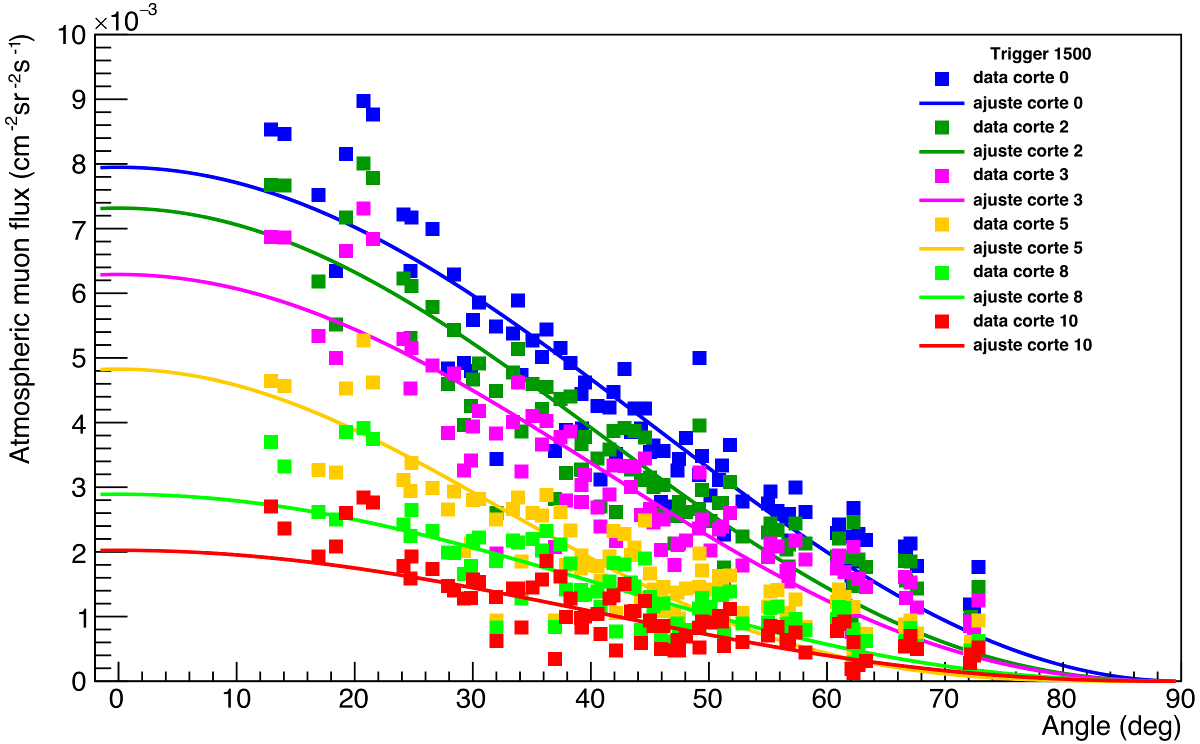

Atmospheric muon flux distribution with respect to the zenith angle (8 hours)

CONCLUSIONS

- For the first time in Peru, a project is being developed regarding muon tomography, of great importance due to its applications in geophysics and archaeology
- The detector channels are capable of capturing charged components of the Extensive Air Showers.
- The detector determines a variety of trajectories, each with a respective zenith angle (depending on the inclination of the detector), and an atmospheric muon flux can be obtained for each.
- This first step of detector characterization provides a baseline on which to work. Methods were developed for the analysis of new data in the country and in an environment optimized for analysis such as ROOT.
- The second step show a good improve in detector detection due to optical adaptation.

Stay tuned!